AUT Journal of Mathematics and Computing

AUT J. Math. Comput., 5(1) (2024) 27-38
https://doi.org/10.22060/AJMC.2023.21758.1106

Original Article

Difference potentials method based on LOD splitting technique for nonlinear convection–diffusion equations with interfaces

Mahboubeh Tavakoli Tameh[a], Fatemeh Shakeri*[a]

[a]*Department of Mathematics and Computer Science, Amirkabir University of Technology (Tehran Polytechnic), Iran*

ABSTRACT: In this paper, we construct a difference potentials method (DPM) based on the locally one-dimensional (LOD) technique to solve the two-dimensional nonlinear convection-diffusion interface problems. The advantage of using the LOD scheme is that the linear system resulting from the auxiliary problem has a simpler structure and can be solved efficiently and accurately with less central processor (CPU) time. Numerical results validate the robustness, accuracy, and efficiency of the proposed method.

Review History:
Received:12 September 2022
Revised:04 April 2023
Accepted:05 April 2023
Available Online:01 January 2024

Keywords:
Difference potentials
Finite difference method
Spectral method
Interface problems

AMS Subject Classification (2010):
65M06; 65M70; 82C24

1. Introduction

The difference potentials method is an efficient and strong technique for solving interface problems and problems defined on domains with complex geometry. This method was proposed by V. Ryaben'kii in 1969 and is a discrete counterpart of Calderon's potential theory in the functional analysis [13, 14]. It combines some advantages of the boundary element method (BEM) and finite difference method (FDM) while avoiding some drawbacks related to them. The advantages are the effectiveness of the FDM in simple geometries and the dimension reduction of the BEM. The avoided drawbacks by this method include the difficulty of the FDM in handling complex regions and the requirement of the BEM to the fundamental solution and evaluation of the singular integral kernels [7]. In the DPM, first, the value of the solution is calculated at the discrete grid boundary (the grid points close to the boundaries of the original domains) by constructing pseudo-differential boundary equations [1, 3, 4, 5, 6, 10, 11, 12, 15, 19]. Then, these values are used in the discrete generalized Green's formula to obtain the values of the solution in the original domain. In the difference potentials method, the partial derivation discretization is performed by the finite difference method and implicit finite difference schemes have often been used for discretization in the previous

*Corresponding author.
E-mail addresses: mh.tavakoli@aut.ac.ir, f.shakeri@aut.ac.ir

stages of the development of this method. Implicit schemes are popular for time-dependent problems. However, one drawback of these methods is the need to solve a large system of equations in multidimensional problems, which are more time-consuming (computationally expensive). One treatment for this problem may be the use of the splitting techniques, such as the LOD method, which replaces the multidimensional equations with a sequence of one-dimensional equations. Therefore, at each time level, we solve a sequence of tridiagonal systems, which have a simpler structure [2, 16, 18]. In this paper, our aim is to design a difference potentials method based on the LOD technique to solve the nonlinear convection-diffusion interface problems.

We consider the following nonlinear convection-diffusion equation defined in the interface domain $\Omega = \Omega_1 \cup \Omega_2$:

$$u_t + uu_x + uu_y = \mu[u_{xx} + u_{yy}] + f, \qquad (x, y, t) \in \Omega \times (0, T], \tag{1}$$

with the initial condition as

$$u(x, y, 0) = u^0(x, y), \qquad (x, y) \in \Omega,$$

boundary condition on the exterior boundary $\partial\Omega_1$ as

$$u(x, y, t) = k(x, y, t), \qquad (x, y, t) \in \partial\Omega_1 \times (0, T],$$

and interface conditions on $\Gamma = \Omega_1 \cap \Omega_2$ in the following forms

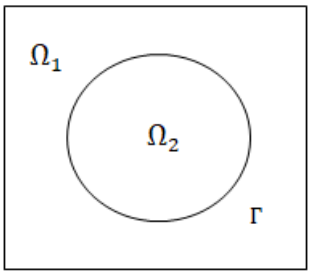

Figure 1: Computational domain Ω with interior domain Ω_2, exterior domain Ω_1 and interface Γ.

$$[u]_\Gamma = g_1(x, y, t), \qquad (x, y) \in \Gamma, \quad t \in (0, T], \tag{2}$$

$$[\mu u_{\mathbf{n}}(x, y)]_\Gamma = g_2(x, y), \qquad (x, y) \in \Gamma, \quad t \in (0, T], \tag{3}$$

where $\Omega \subset \mathbb{R}^2$ is a bounded domain separated by an interface Γ into two disjoint subdomains Ω_1 and Ω_2 and $\mathbf{n} = (n_1, n_2)$ is the unit normal vector to Γ pointing outward. The jump, $[.]_\Gamma$, is defined as the difference of the limiting values from two different sides of the interface.

$$[u]_\Gamma = \lim_{\substack{(x,y)\to\Gamma \\ (x,y)\in\Omega_1}} u(x, y) - \lim_{\substack{(x,y)\to\Gamma \\ (x,y)\in\Omega_2}} u(x, y).$$

The velocity coefficient μ and source function f are piecewise smooth but can have a jump along the interface Γ, hence the solution of this problem may be discontinuous along Γ.

2. LOD-DPM algorithm

In this section, we describe the main steps of the DPM algorithm based on the LOD scheme for governing interface problems. From now on, we use superscript $e \in \{1, 2\}$ to distinguish between subdomains Ω_1 and Ω_2 and the concepts related to them.

2.1. Auxiliary domain

First, we embed each subdomain Ω_e, which may have an irregular shape, in a large and simple auxiliary domain Ω_e^0 such as a rectangle. Then, we define a uniform Cartesian grid N_e^0 on this auxiliary domain and consider a finite-difference stencil that is convenient for creating a method with the desired accuracy. Here, we select the following 5-node stencil $N_{i,j}^5$ to design a second-order method

$$N_{i,j}^5 = \{(x_i, y_j), (x_{i\pm1}, y_j), (x_i, y_{j\pm1})\}.$$

Next, we define the point sets M_e^0, M_e^+, M_e^-, N_e^0, N_e^+, N_e^- and γ_e for each auxiliary subdomain, that we will use in the difference potentials framework as bellow

- $M_e^0 = \{(x_i, y_j) | (x_i, y_j) \in \Omega_e^0\}$
- $M_e^+ = \{(x_i, y_j) | (x_i, y_j) \in \Omega_e\}$
- $M_e^- = \{(x_i, y_j) | (x_i, y_j) \in M_e^0 \setminus M_e^+\}$
- $N_e^+ = \{\cup N_{i,j}^5 \mid (x_i, y_j) \in M_e^+\}$,
- $N_e^- = \{\cup N_{i,j}^5 \mid (x_i, y_j) \in M_e^-\}$,
- $N_e^0 = \{\cup N_{i,j}^5 \mid (x_i, y_j) \in M_e^0\}$,
- $\gamma_e = N_e^+ \cap N_e^-$.

2.2. LOD finite difference discretization

Since one-dimensional equations are easier to solve than two-dimensional equations, we apply a LOD strategy that splits (1) to the following one-dimensional equations

$$\frac{1}{2}u_t + uu_x = \mu u_{xx} + \frac{1}{2}f, \qquad t \in [t^n, t^{n+1/2}], \tag{4}$$

$$\frac{1}{2}u_t + uu_y = \mu u_{yy} + \frac{1}{2}f, \qquad t \in [t^{n+1/2}, t^{n+1}], \tag{5}$$

Then, we can apply the schemes used for solving the 1D nonlinear convection-diffusion equation to solve (4) and (5). In this work, we use the Euler method to linearize these equations and second-order central finite difference scheme methodologies for discretizing them in the following form

$$L_{\Delta t,h}^{(1)}[u_{i,j}^{n+1/2}] = F_{i,j}^{n+1/2}, \qquad t \in [t^n, t^{n+1/2}], \tag{6}$$

$$L_{\Delta t,h}^{(2)}[u_{i,j}^{n+1}] = F_{i,j}^{n+1}, \qquad t \in [t^{n+1/2}, t^{n+1}], \tag{7}$$

where $L_{\Delta t,h}^{(1)}[u_{i,j}^{n+\frac{1}{2}}]$ and $L_{\Delta t,h}^{(2)}[u_{i,j}^{n+1}]$ are operators defined by

$$L_{\Delta t,h}^{(1)}[u_{i,j}^{n+\frac{1}{2}}] = (1 - \Delta t {\delta_x}^2)u_{i,j}^{n+\frac{1}{2}}, \qquad L_{\Delta t,h}^{(2)}[u_{i,j}^{n+1}] = (1 - \Delta t {\delta_y}^2)u_{i,j}^{n+1},$$

and the right-hand side in (6) and (7) take the forms as come in below

$${F_{i,j}}^{n+\frac{1}{2}} = \Delta t f^{n+\frac{1}{2}} + (1 - \Delta t \delta_x u^n)u^n,$$

$${F_{i,j}}^{n+1} = \Delta t f^{n+1} + (1 - \Delta t \delta_y u^{n+\frac{1}{2}})u^{n+\frac{1}{2}},$$

in which, Δt is the time step, $\Delta x = \Delta y = h$ are space steps in x- and y-axis directions, respectively. Also, δ_x, δ_x^2, δ_y, δ_y^2, are the partial derivatives discretized by following central finite difference schemes

$$\delta_x u_{i,j} = \frac{u_{i+1,j} - u_{i-1,j}}{2\Delta x},$$

$$\delta_y u_{i,j} = \frac{u_{i,j+1} - u_{i,j-1}}{2\Delta y},$$

$$\delta_x^2 u_{i,j} = \frac{u_{i+1,j} - 2u_{i,j} + u_{i-1,j}}{\Delta x^2},$$

$$\delta_y^2 u_{i,j} = \frac{u_{i,j+1} - 2u_{i,j} + u_{i,j-1}}{\Delta y^2},$$

2.3. Stability, Error Analysis and Convergence of the Scheme

Now, we illustrate the stability and the order of convergence for the proposed method. Without loss of generality, here, we set $\mu = 1$.

Stability

We study the stability of the designed scheme via the Von Neumann method that linearizes the nonlinear term and suggests stability. However, the applying the linear stability analysis to nonlinear equations cannot be strongly justified, but it peresents the necessary conditions for stability, which is effective in practice [8, 20].

Theorem 2.1. *Difference equations (6)- (7) are unconditionally stable.*

Proof. See the Appendix, Proof of the Theorem 2.1. □

Error Analysis and Convergence

The modified equation technique, introduced by Warming and Hyett [19], is a strong tool for the analysis of the accuracy of a numerical method with the aim of solving a time-dependent problem governed by a partial differential equation.

Theorem 2.2. *For two-dimensional nonlinear convection–diffusion problem (1)–(3), if $u \in C^3(\Omega)$ and initial condition is given by (1), then the difference scheme (6)–(7) is one and two-order convergent in time and space directions in maximum norm, respectively.*

Proof. See the Appendix, Proof of the Theorem 2.2. □

Theorem 2.3. *Difference equations (6)- (7) are convergent.*

Proof. See the Appendix, Proof of the Theorem 2.3. □

2.4. Auxiliary problem (AP) and the boundary equations with projections (BEP)

Now, for each time level $t^{n+k/2}, k \in \{1, 2\}$, we define the discrete auxiliary problem in each auxiliary domain Ω_e^0 as the solution of the following system of equations

$$L^{(k)}_{\Delta t,h}[u^{n+k/2}_{i,j}] = q^{n+k/2}_{i,j}, \qquad (x_i, y_j) \in M^0_e, \tag{8}$$

$$u^{n+k/2}_{i,j} = 0, \qquad (x_i, y_j) \in N^0_e \backslash M^0_e, \tag{9}$$

where $q^{n+k/2}_{i,j}$ is a grid function defined on M^0_e.
Note that, for the first step from t^n to $t^{n+1/2}$ superscript k is equal to 1 and for the second step from $t^{n+1/2}$ to t^{n+1}, it is equal to 2.

Now, we construct the particular solution and difference potential with the help of the auxiliary problem.

Definition 2.4. *At each time level $t^{n+k/2}$, the particular solution of the problem for each subdomain Ω_e is defined as the solution (restricted on N^+_e) of the auxiliary problem (8)-(9) with the following right-hand side*

$$q^{n+k/2}_{i,j} = \begin{cases} F^{n+k/2}_{i,j}, & (x_i, y_j) \in M^+_e, \\ 0, & (x_i, y_j) \in M^-_e. \end{cases}$$

If we introduce $G^{(k)}_{\Delta t,h}$ as the inverse operator of $L^{(k)}_{\Delta t,h}$, we can display this solution as $u^{n+k/2}_{i,j} = G^{(k)}_{\Delta t,h} F^{n+k/2}_{i,j}$.

Definition 2.5. *At each time level $t^{n+k/2}$ and for each subdomain Ω_e, the difference potential with density $v^{n+k/2}_{\gamma_e} \in V_{\gamma^e}$ is defined as the grid function $u^{n+k/2}_{i,j} = P^{(k)}_{N^+_e} v^{n+k/2}_{\gamma_e}$, and coincides with the solution (restricted on N^+_e) of the auxiliary problem (8)-(9) with the following right hand side*

$$q^{n+k/2}_{i,j} = \begin{cases} 0, & (x_i, y_j) \in M^+_e, \\ L^{(k)}_{\Delta t,h}[v^{n+k/2}_{\gamma^e}], & (x_i, y_j) \in M^-_e. \end{cases}$$

Here, V_{γ^e} is introduced as a linear space of all grid functions denoted on γ_e. We will extend the value of these functions by zero to other points of the grid N^0_e.
$P^{(k)}_{N^+_e} : V_{\gamma_e} \to N^+_e$ is a linear operator, which represents the value of the difference potential from the density v_{γ_e} and can be easily constructed [14].

Now, we state the main theorem of DPM for interface problems [1].

Theorem 2.6. *Discrete density* $u_\gamma^{n+k/2} := (u_{\gamma_1}^{n+k/2}, u_{\gamma_2}^{n+k/2})$ *is the trace of some solution* $u^{n+k/2}$ *to the difference equations (6)/(7), i.e.* $u_\gamma^{n+k/2} = Tr_\gamma u^{n+k/2}$*, iff, the following hybrid system of boundary equations with projections holds*

$$(I - P_{\gamma_1^+}^{(k)})u_{\gamma_1}^{n+k/2} = G_{\Delta t,h}^{(k)} F_{\gamma_1}^{n+k/2}, \qquad (x_i, y_j) \in \gamma_1, \tag{10}$$

$$(I - P_{\gamma_2^+}^{(k)})u_{\gamma_2}^{n+k/2} = G_{\Delta t,h}^{(k)} F_{\gamma_2}^{n+k/2}, \qquad (x_i, y_j) \in \gamma_2, \tag{11}$$

where $P_{\gamma_e^+}^{(k)}$ *is the trace of the difference potential operator* $P_{N_e^+}^{(k)}$ *on the grid boundary* γ_e*.*

2.5. Extension operator

In DPM, to guarantee the uniqueness of the solution $u_\gamma^{n+k/2} := (u_{\gamma_1}^{n+k/2}, u_{\gamma_2}^{n+k/2})$, the interface and boundary conditions are imposed in BEP by the extension operator Ex. This operator represents the densities $u_{\gamma_e}^{n+k/2}$ with the desired accuracies through the values of the Cauchy data, which is defined as two-component functions $\mathbf{u}_\Gamma^{n+k/2} = (u^{n+k/2}\,|_\Gamma, \frac{\partial u^{n+k/2}}{\partial \mathbf{n}}\,|_\Gamma)$. In the definition of Cauchy data, $u^{n+k/2}\big|_\Gamma$ and $\frac{\partial u^{n+k/2}}{\partial \mathbf{n}}\Big|_\Gamma$ are the trace of the solution $u^{n+k/2}$ and its normal derivative on the interface Γ, respectively,

$$u_{\gamma_e}^{n+k/2} = Ex[\mathbf{u}_\Gamma^{n+k/2}] = Ex(u^{n+k/2}\,|_\Gamma, \frac{\partial u^{n+k/2}}{\partial \mathbf{n}}\,|_\Gamma) = \sum_{l=0}^{L} \frac{d^l}{l!} \frac{\partial^l u^{n+k/2}}{\partial \mathbf{n}^l}\,|_\Gamma, \tag{12}$$

where d denotes the signed distance from the intended point in γ_e to the nearest boundary point on the interface Γ. The higher-order derivatives $\frac{\partial^l u}{\partial r^l}, l = 2, 3, ...$ can be obtained through the Cauchy data and the consecutive differentiation of the governing differential equation with respect to $\mathbf{n}$.

2.6. Unknown unification by spectral approach

To incorporate extension operators (12) with interface conditions (2)-(3) simplicity and efficiency, we use the spectral approach for approximating the unknown terms $u^{n+k/2}\big|_\Gamma$ and $\frac{\partial u^{n+k/2}}{\partial \mathbf{n}}\Big|_\Gamma$ on the continuous boundary Γ. So, we can write an expansion for $\boldsymbol{u}_\Gamma^{n+k/2}$ with respect to some basis $\{\Psi_j^0 = (\psi_j^0, 0), \Psi_j^1 = (0, \psi_j^1), \quad j = 0, ..., M\}$ chosen on Γ as

$$\mathbf{u}_\Gamma^{n+k/2} \approx \sum_{j=0}^{M} \alpha_j^{e,n+k/2} \Psi_j^0 + \sum_{j=0}^{M} \beta_j^{e,n+k/2} \Psi_j^1. \tag{13}$$

where ψ_j^0 and $\psi_j^1, j = 0, ..., M$ are spectral basis functions.
By employing extension (12) in (13) and placing it in (10)-(11), this coupled system is reduced to the following form

$$\sum_{j=0}^{M} \alpha_j^{1,n+k/2}(I - P_{\gamma_1^+}^{(k)})Ex(\Psi_j^0) + \sum_{j=0}^{M} \beta_j^{1,n+k/2}(I - P_{\gamma_1^+}^{(k)})Ex(\Psi_j^1) = G_{\Delta t,h}^{(k)} F_{\gamma_1}^{n+k/2},$$

$$\sum_{j=0}^{M} \alpha_j^{2,n+k/2}(I - P_{\gamma_2^+}^{(k)})Ex(\Psi_j^0) + \sum_{j=0}^{M} \beta_j^{2,n+k/2}(I - P_{\gamma_2^+}^{(k)})Ex(\Psi_j^1) = G_{\Delta t,h}^{(k)} F_{\gamma_2}^{n+k/2}.$$

which is an overdetermined system and can be solved by the least square method to calculate the unknowns $\alpha_j^{e,n+k/2}$ and $\beta_j^{e,n+k/2}$. Now we can reconstruct $\mathbf{u}_\Gamma^{n+k/2}$ with the help of (13) and obtain $u_{\gamma_e}^{n+k/2}$ using (12).

2.7. Discrete Green's formula

At the end step of DPM, we obtain the approximate solution $u_{i,j}^{n+k/2}$ of the exact solution $u(x_i, y_j, t^{n+k/2})$ in N_e^+ by substituting the computed density $u_{\gamma_e}^{n+k/2}$ in discrete Green's formula:

$$u_{i,j}^{n+k/2} = P_{N_e^+}^{(k)} u_{\gamma_e}^{n+k/2} + G_{\Delta t,h}^{(k)} F_{i,j}^{n+k/2}, \qquad (x_i, y_j) \in \Omega_e.$$

3. Numerical results

In this section, we present some numerical examples to show the performance and accuracy of the proposed method for solving the nonlinear convection-diffusion interface problem. For all cases, the exterior domain is $\Omega_1 = [-1,1] \times [-1,1] \setminus \Omega_2$. For test example 2, we select Ω_2 as a domain with an ellipse-shaped boundary centered at the origin, $\Omega_2 = \{(x,y) : \frac{x^2}{a^2} + \frac{y^2}{b^2} < 1\}$ and for other test examples, we consider the interior domain as a disk of radius r_0 centered at the origin, $\Omega_2 = \{(x,y) : x^2 + y^2 < r_0^2\}$. We select the auxiliary domain as a square whose boundary coincides with the exterior boundary $\partial\Omega_1$ for both exterior and interior domains. Since the exact solution is known, we calculate the source term, Dirichlet boundary conditions on the exterior boundary, and interface jump conditions on the interface Γ according to the given exact solution. Here, we select Fourier basis functions $\psi_0(\theta) = 1, \psi_{2j}(\theta) = \sin(\frac{2\pi j}{|\Gamma|}\theta), \psi_{2j+1}(\theta) = \cos(\frac{2\pi j}{|\Gamma|}\theta), j = 1,2,...,M$ for the spectral approximation. Also, we consider $\Delta t = h^2$ and time interval $[0,T]$ with $T = 3$ as the final time.

Note that the number of basis functions M is selected grid-independent. It means that M is selected in such a way that the error of spectral approximation on Γ is smaller than the error that we expect to obtain on all grids.

Designed algorithm is implemented with MATLAB running on a desktop with Intel(R) Core(TM) i7-9700M CPU @ 3.00GHz 3.00 GHz and 16 GB memory.

3.1. Test example1

The exact solution of this example is given by

$$u(x,y) = \begin{cases} \cos(t)\sin(\frac{\pi}{4}(x+1))\sin(\frac{\pi}{4}(y+1)), & in\ \ \Omega_1, \\ 1, & in\ \ \Omega_2, \end{cases} \tag{14}$$

and $\mu_1 = \mu_2 = 1$. The interface Γ is a circle of radius $r_0 = \frac{1}{2}$. We compare the obtained results of LOD-DPM with the results of the DPM in which the governing equation is discretized with the central finite difference schemes. The grid refinement analysis of this example is reported in Table 1 and Fig. 2, which provide a second-order accuracy in space for the designed methods. Also, it can be found that the numerical solution of LOD-DPM is almost similar to the numerical solution of DPM, but we see that the LOD-DPM is more efficient and takes less computational time.

Table 1: Numerical results and consuming time of LOD-DPM and DPM with the number of basis functions M = 15 for the example 1.

	LOD-DPM			DPM		
N	Error	order	CPU time (s)	Error	order	CPU time (s)
40	4.4614e-04	*	5.005395	1.6701e-04	*	5.061699
80	1.1656e-04	1.9364	31.830595	4.0831e-05	2.0322	78.559320
160	2.9630e-05	1.9759	367.520962	1.0099e-05	2.0149	1.4750e+03
320	7.4649e-06	1.9889	5.2047e+03	2.4895e-06	2.0203	3.4047e+04

3.2. Test example2

In this test example, the exact solution is defined as

$$u(x,y,t) = \begin{cases} \exp(-t)\exp(x)\cos(\frac{\pi y}{2}), & in\ \ \Omega_1, \\ \exp(-t)(-8x^2 - 8y^2 + \frac{7}{2}), & in\ \ \Omega_2, \end{cases} \tag{15}$$

and $\mu_1 = \mu_2 = 1$. The interface Γ is an ellipse with $a = \frac{18}{27}$ and $b = \frac{10}{27}$. The numerical results of this example are reported in Table 2 and the plot of the approximate solution on a 40×40 mesh is shown in Fig. 3. We see that the LOD-DPM is more efficient than the DPM under guaranteeing the sufficient accuracy of numerical solutions for solving the governing equation in the domain with the ellipse-shaped interface.

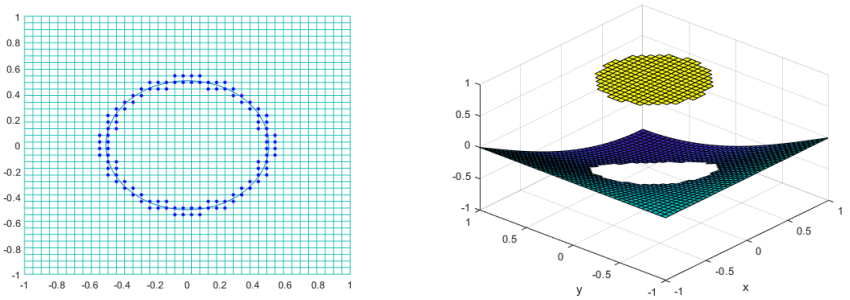

(a) (b)

Figure 2: The grid boundary γ (left), and plot of the numerical solution (right) on a 40×40 grid for the example 1.

Table 2: Numerical results and consuming time of LOD-DPM and DPM with the number of basis functions M = 15 for the example 2.

	LOD-DPM			DPM		
N	Error	order	CPU time (s)	Error	order	CPU time (s)
40	4.9800e-04	*	3.999805	4.4624e-04	*	5.498760
80	1.3186e-04	1.9171	31.851611	1.5207e-04	1.5531	89.672682
160	3.4904e-05	1.9175	371.705234	3.4854e-05	2.1253	1592.270996
320	8.7772e-06	1.9916	5.3993e+03	9.4398e-06	1.8845	4.0598e+04

3.3. Test example3

In this test example, the exact solution is defined as

$$u(x,y,t) = \begin{cases} -\exp(-t)(1+\ln(2r)), & in\ \ \Omega_1, \\ -\exp(-t), & in\ \ \Omega_2, \end{cases} \tag{16}$$

and, the interface Γ is a circle of radius $r_0 = \frac{1}{2}$. We consider this example but with some typical different jump ratios for μ. The numerical results, reported in Tables (3)-(5), show the similar convergence for all different cases and confirm the flexibility of the designed method in dealing with interface problems with more chalenges.

Table 3: The numerical convergence rate and error for example 3.

	$\mu 1 = 5,\ \mu 2 = 1$		$\mu 1 = 1,\ \mu 2 = 5$	
	LOD-DPM		LOD-DPM	
N	E	order	E	order
20	$9.6144e-04$	*	00.0050	*
40	$3.1097e-04$	1.6284	0.0016	1.6439
80	$7.8229e-05$	1.9910	$5.0243e-04$	1.6711
160	$2.0028e-05$	1.9657	$1.3489e-04$	1.8971

3.4. Test example 4

In this example we consider the exact solutions (14), (15) and (16). Then we compare the results of the presented method with the results of immersed interface method that are reported in [9]. Here, the interface is a circle with radius $r_0 = \frac{1}{2}$ as considered in that work.

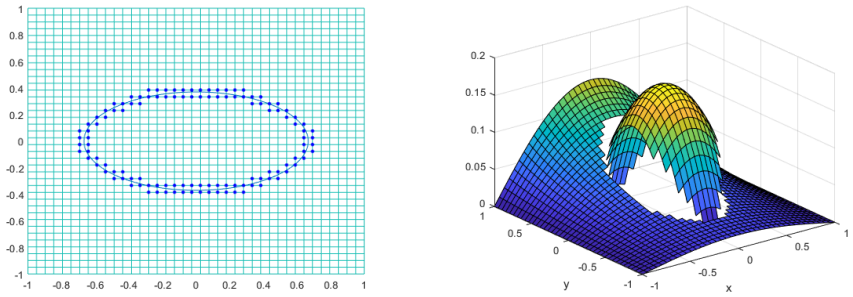

(a) (b)

Figure 3: The grid boundary γ (left), and plot of the numerical solution (right) on a 40×40 grid for the example 2.

Table 4: The numerical convergence rate and error for example 3.

	$\mu1 = 10,\ \mu2 = 1$		$\mu1 = 1,\ \mu2 = 10$	
	LOD-DPM		LOD-DPM	
N	E	order	E	order
20	$5.7830e-04$	$*$	0.0051	$*$
40	$1.8711e-04$	1.6279	0.0014	1.8651
80	$5.4161e-05$	1.7886	$3.5583e-04$	1.9762
160	$1.4060e-05$	1.9457	$8.5895e-05$	2.0505

We see that the results obtained by the difference potentials method are close to the results reported in [9]. However LOD-DPM has some advantages in comparison with IIM. For example, LOD-DPM does not face the challenge of reducing the order of accuracy in the points that surround the interface Γ (irregular points in IIM) so in contrast to IIM, LOD-DPM doesn't need to correct the finite difference schemes in these points. Also, applying interface conditions in LOD-DPM, especially in the circle interfaces, is done with a simple strategy without defining a local coordinate system that is required in IIM to calculate the jump conditions and correction terms. In addition, detecting interface Γ is done with the level set function in IIM as presented in [9], but we see that LOD-DPM does not need this technique, and the coordinates of the nearest point on the interface to each point of the discrete boundary grid γ, which is required in the extension operator, can be easily calculated using the coordinates of the same grid nodes of γ.

4. Conclusion

In this work, the difference potentials method was successfully developed for solving the nonlinear convection-diffusion interface problem. The governing equation is discretized on a regular structured grid, which guarantees no loss of accuracy for non-conforming interfaces. Also, the LOD finite difference scheme was used to improve the computational efficiency of the DPM. The conducted numerical experiment illustrates the capability and second-order accuracy of the proposed method for this problem.

Conflict of interest

On behalf of all authors, the corresponding author states that there is no conflict of interest.

Appendix

Proofs of the Theorems.

Table 5: The numerical convergence rate and error for example 3.

	$\mu1 = 100$, $\mu2 = 1$		$\mu1 = 1$, $\mu2 = 100$	
	LOD-DPM		LOD-DPM	
N	E	order	E	order
20	0.0374	*	0.0277	*
40	0.0052	2.8465	0.0114	1.2809
80	0.0013	2	0.0038	1.5850
160	$2.0286e-04$	2.6800	0.001	1.9260

Table 6: The comparison of the error and convergence rate of LOD-DPM with the results of IIM in the final time $T = 3$ for the exact solution (14).

	LOD-DPM		IIM	
N	Error	order	Error	order
20	1.5128e-03	*	2.8923e-03	*
60	2.0433e-04	1.8222	3.1392e-04	2.0213
100	7.5085e-05	1.9597	1.1239e-04	2.0107

Table 7: The comparison of the error and convergence rate of LOD-DPM with the results of IIM in the final time $T = 3$ for the exact solution (15).

	LOD-DPM		IIM	
N	Error	order	Error	order
20	0.0028	*	7.1082e-04	*
60	2.5346e-04	2.1865	7.9219e-05	1.9972
100	8.6445e-05	2.1058	2.8298e-05	2.4924

Table 8: The comparison of the error and convergence rate of LOD-DPM with the results of IIM in the final time $T = 3$ for the exact solution (16).

	LOD-DPM		IIM	
N	Error	order	Error	order
20	5.3333e-04	*	3.7163e-04	*
60	5.8969e-05	2.0045	4.4433e-05	1.9333
100	2.4520e-05	1.7179	1.5404e-05	2.0738

Proof of the Theorem 2.1.

We consider the equations (6)-(7). If we set u^n or $u^{n+\frac{1}{2}}$ as the initial conditions in the nonlinear terms, the error terms of these two equations can be written as

$$(1 - \Delta t {\delta_x}^2)\mathbf{e}_{i,j}^{n+\frac{1}{2}} = \mathbf{e}_{i,j}^{n}, \tag{17}$$

$$(1 - \Delta t {\delta_y}^2)\mathbf{e}_{i,j}^{n+1} = \mathbf{e}_{i,j}^{n+\frac{1}{2}}.$$

To show the Von Neumann stability of the designed scheme, we replace

$$\mathbf{e}_{i,j}^{n} = \mathbf{e}_{p,q}^{r} = G^r e^{i\beta ph} e^{i\beta qk},$$

since $\triangle x = \triangle y = h$, we set

$$\mathbf{e}_{p,q}^{r} = G^r e^{i\beta ph} e^{i\beta qh},$$

where $i=\sqrt{-1}$ and G is often called amplification factor. The proposed scheme will be stable if $|G|\leq 1$. First we consider (17), so we have

$$(1+s)G^{r+1/2}e^{i\beta ph}e^{i\beta qh}-\frac{s}{2}G^{n+1/2}e^{i\beta(p-1)h}e^{i\beta qh}-\frac{s}{2}G^{n+1/2}e^{i\beta(p+1)h}e^{i\beta qh}=G^{n}e^{i\beta ph}e^{i\beta qh}, \tag{18}$$

where $s=\frac{2\triangle t}{h^2}$. The division equation (18) by $G^{r}e^{i\beta ph}e^{i\beta qh}$ can be written as

$$(1+s)G^{1/2}-\frac{s}{2}G^{1/2}e^{-i\beta h}-\frac{s}{2}G^{1/2}e^{i\beta h}=1,$$

and then

$$\begin{aligned}G^{1/2}&=\frac{1}{1+s-s/2e^{-i\beta h}-s/2e^{i\beta h}}\\&=\frac{1}{1+s-s/2(\cos(\beta h)-i\sin(\beta h))-s/2(\cos(\beta h)+i\sin(\beta h))}\\&=\frac{1}{1+s-s\cos(\beta h)}=\frac{1}{1+s(1-\cos(\beta h))}\\&=\frac{1}{1+2s\sin^2(\beta h/2)}.\end{aligned}$$

To obtain the stability, it is enough to show $|G|\leq 1$, which clearly holds. Similarly, for (4), we can show that $|G|\leq 1$. So, the schemes (6)-(7) are unconditionally stable.

Proof of the Theorem 2.2.
For the solution of (6)–(7), i, j and n are the spatial (x- and y-axis) and temporal indices respectively, $\Delta x=\Delta y=h$ and Δt are the mesh size and the time step, so that $u_{i,j}^{n}$ is an approximation of $u(i\Delta x,j\Delta y,n\Delta t)$. The modified equation for the scheme (6) is a formal partial differential equation, which is derived from the difference equation:

$$(u_{i,j}^{n+1/2}-u_{i,j}^{n})=M3-M1-M2 \tag{19}$$

where

$$\begin{aligned}M1&=\frac{s}{2}(u_{i,j}^{n+1/2}-u_{i-1,j}^{n+1/2}),\\M2&=\frac{s}{2}(u_{i,j}^{n+1/2}-u_{i+1,j}^{n+1/2}),\\M3&=-\frac{\Delta t}{2h}u_{i,j}^{n}(u_{i+1,j}^{n}-u_{i-1,j}^{n})+\frac{\Delta t}{2}f_{i,j}^{n+1/2}\end{aligned}$$

We can write for each part of (19), the following Taylor expansions at the point with indices (i,j,n)

$$(u_{i,j}^{n+1/2}-u_{i,j}^{n})=[u|_{i,j}^{n}+\frac{\Delta t}{2}\frac{\partial u}{\partial t}|_{i,j}^{n}+(\frac{\Delta t}{2})^2\frac{\partial^2 u}{\partial t^2}|_{i,j}^{n}+\ldots-u|_{i,j}^{n}]=\frac{\Delta t}{2}\frac{\partial u}{\partial t}|_{i,j}^{n}+O(\Delta t^2), \tag{20}$$

$$M1=\frac{s}{2}[u|_{i,j}^{n}-(u|_{i,j}^{n}-h\frac{\partial u}{\partial x}|_{i,j}^{n}+\frac{h^2}{2}\frac{\partial^2 u}{\partial x^2}|_{i,j}^{n}-\frac{h^3}{3!}\frac{\partial^3 u}{\partial x^3}|_{i,j}^{n}+\frac{h^4}{4!}\frac{\partial^4 u}{\partial x^4}|_{i,j}^{n}+\ldots)+O(\Delta t)], \tag{21}$$

$$M2=\frac{s}{2}[u|_{i,j}^{n}-(u|_{i,j}^{n}+h\frac{\partial u}{\partial x}|_{i,j}^{n}+\frac{h^2}{2}\frac{\partial^2 u}{\partial x^2}|_{i,j}^{n}+\frac{h^3}{3!}\frac{\partial^3 u}{\partial x^3}|_{i,j}^{n}+\frac{h^4}{4!}\frac{\partial^4 u}{\partial x^4}|_{i,j}^{n}+\ldots)+O(\Delta t)], \tag{22}$$

$$\begin{aligned}M3=-\frac{\Delta t}{2h}u|_{i,j}^{n}[(u|_{i,j}^{n}+h\frac{\partial u}{\partial x}|_{i,j}^{n}+\frac{h^2}{2}\frac{\partial^2 u}{\partial x^2}|_{i,j}^{n}+\frac{h^3}{3!}\frac{\partial^3 u}{\partial x^3}|_{i,j}^{n}+\frac{h^4}{4!}\frac{\partial^4 u}{\partial x^4}|_{i,j}^{n}+\ldots-u|_{i,j}^{n})+(u|_{i,j}^{n}-u|_{i,j}^{n}+\\h\frac{\partial u}{\partial x}|_{i,j}^{n}-\frac{h^2}{2}\frac{\partial^2 u}{\partial x^2}|_{i,j}^{n}+\frac{h^3}{3!}\frac{\partial^3 u}{\partial x^3}|_{i,j}^{n}-\frac{h^4}{4!}\frac{\partial^4 u}{\partial x^4}|_{i,j}^{n}+\ldots)]+\frac{\Delta t}{2}(f|_{i,j}^{n}+O(\Delta t))\end{aligned} \tag{23}$$

Now if we replace (20)-(23) in (19) and taking into account $s=\frac{2\triangle t}{h^2}$ we have

$$\frac{1}{2}\frac{\partial u}{\partial t}-\frac{\partial^2 u}{\partial x^2}-\frac{h^2}{12}\frac{\partial^4 u}{\partial x^4}+u\frac{\partial u}{\partial x}-\frac{h^2}{3!}\frac{\partial^3 u}{\partial x^3}+\frac{1}{2}f+O(\Delta t)=0,$$

or in the equivalent form

$$\frac{1}{2}\frac{\partial u}{\partial t}-\frac{\partial^2 u}{\partial x^2}+u\frac{\partial u}{\partial x}+\frac{1}{2}f+O(\Delta t)+O(h^2)=0.$$

It is readily seen that the local truncation error of (6) is $O(\Delta t+h^2)$. In a similar way, we can show that the local truncation error of (7) is $O(\Delta t+h^2)$.

Proof of the Theorem 2.3.

From the derivation process of the scheme, Theorem 2.1 and Theorem 2.2, it is readily seen that the proposed scheme is consistent and unconditionally stable. Therefore we can announce that the proposed schemes is convergent by the Lax equivalence theorem [17].

References

[1] J. Albright, Y. Epshteyn, M. Medvinsky, and Q. Xia, *High-order numerical schemes based on difference potentials for 2D elliptic problems with material interfaces*, Appl. Numer. Math., 111 (2017), pp. 64–91.

[2] A. R. Appadu and H. H. Gidey, *Time-splitting procedures for the numerical solution of the 2d advection-diffusion equation*, Mathematical Problems in Engineering, 2013 (2013), p. 634657.

[3] D. S. Britt, S. V. Tsynkov, and E. Turkel, *A high-order numerical method for the Helmholtz equation with nonstandard boundary conditions*, SIAM J. Sci. Comput., 35 (2013), pp. A2255–A2292.

[4] S. Britt, S. Petropavlovsky, S. Tsynkov, and E. Turkel, *Computation of singular solutions to the Helmholtz equation with high order accuracy*, Appl. Numer. Math., 93 (2015), pp. 215–241.

[5] Y. Epshteyn, *Upwind-difference potentials method for Patlak-Keller-Segel chemotaxis model*, J. Sci. Comput., 53 (2012), pp. 689–713.

[6] Y. Epshteyn and M. Medvinsky, *On the solution of the elliptic interface problems by difference potentials method*, in Spectral and high order methods for partial differential equations—ICOSAHOM 2014, vol. 106 of Lect. Notes Comput. Sci. Eng., Springer, Cham, 2015, pp. 197–205.

[7] S. Huang and Y. Liu, *A fast multipole boundary element method for solving the thin plate bending problem*, Eng. Anal. Bound. Elem., 37 (2013), pp. 967–976.

[8] E. Lee and D. Kim, *Stability analysis of the implicit finite difference schemes for nonlinear Schrödinger equation*, AIMS Math., 7 (2022), pp. 16349–16365.

[9] J. Liu and Z. Zheng, *IIM-based ADI finite difference scheme for nonlinear convection-diffusion equations with interfaces*, Appl. Math. Model., 37 (2013), pp. 1196–1207.

[10] M. Medvinsky, S. Tsynkov, and E. Turkel, *The method of difference potentials for the Helmholtz equation using compact high order schemes*, J. Sci. Comput., 53 (2012), pp. 150–193.

[11] ——, *High order numerical simulation of the transmission and scattering of waves using the method of difference potentials*, J. Comput. Phys., 243 (2013), pp. 305–322.

[12] ——, *Solving the Helmholtz equation for general smooth geometry using simple grids*, Wave Motion, 62 (2016), pp. 75–97.

[13] A. A. Reznik, *Approximation of surface potentials of elliptic operators by difference potentials*, Dokl. Akad. Nauk SSSR, 263 (1982), pp. 1318–1321.

[14] V. S. Ryaben'kii, *Method of difference potentials and its applications*, vol. 30 of Springer Series in Computational Mathematics, Springer-Verlag, Berlin, 2002. Translated from the 2001 Russian original by Nikolai K. Kulman.

[15] V. S. Ryaben'kii, V. I. Turchaninov, and E. Y. Èpshteĭn, *An algorithm composition scheme for problems in composite domains based on the method of difference potentials*, Zh. Vychisl. Mat. Mat. Fiz., 46 (2006), pp. 1853–1870.

[16] Q. Sheng, *The legacy of ADI and LOD methods and an operator splitting algorithm for solving highly oscillatory wave problems*, in Modern mathematical methods and high performance computing in science and technology, vol. 171 of Springer Proc. Math. Stat., Springer, Singapore, 2016, pp. 215–230.

[17] G. D. Smith, *Numerical solution of partial differential equations*, Oxford Applied Mathematics and Computing Science Series, The Clarendon Press, Oxford University Press, New York, third ed., 1985. Finite difference methods.

[18] D. A. Voss and A. Q. M. Khaliq, *Parallel LOD methods for second order time dependent PDEs*, Comput. Math. Appl., 30 (1995), pp. 25–35.

[19] R. F. Warming and B. J. Hyett, *The modified equation approach to the stability and accuracy analysis of finite-difference methods*, J. Comput. Phys., 14 (1974), pp. 159–179.

[20] H. Zhu, H. Shu, and M. Ding, *Numerical solutions of two-dimensional Burgers' equations by discrete Adomian decomposition method*, Comput. Math. Appl., 60 (2010), pp. 840–848.

Please cite this article using:

Mahboubeh Tavakoli Tameh, Fatemeh Shakeri, Difference potentials method based on LOD splitting technique for nonlinear convection–diffusion equations with interfaces, AUT J. Math. Comput., 5(1) (2024) 27-38
https://doi.org/10.22060/AJMC.2023.21758.1106